Equilibrium Studies on the Association of the Nuclear Poly(A) Binding Protein with Poly(A) of Different Lengths†

Sylke Meyer,*,‡ Claus Urbanke,§ and Elmar Wahle‡

Institut für Biochemie, Martin-Luther-Universität Halle-Wittenberg, Halle (Saale), Germany, and Zentrale Einrichtung für Biophysikalisch-Biochemische Verfahren, Medizinische Hochschule Hannover, Carl-Neuberg-Strasse 1, 30623 Hannover, Germany

Received December 21, 2001; Revised Manuscript Received March 21, 2002

ABSTRACT: The nuclear poly(A) binding protein (PABPN1) binds the growing poly(A) tail during pre-mRNA 3′-end processing, stimulating its elongation and controlling its final length. Here we report binding studies of PABPN1 to poly(A) in solution. Quantitative fluorescence titration was used to determine the stoichiometry, intrinsic affinity, and cooperativity of binding to a series of size-fractionated poly(A). The intrinsic association constant K_i was about 2×10^6 M^{-1} for oligo(A) and all size classes of poly(A). The binding of PABPN1 to poly(A) was enhanced by protein−protein interactions which were, however, weak (cooperativity parameter $\omega < 50$). No significant change of cooperativity could be detected with increasing polynucleotide length in the range of 140−450 nucleotides. An average binding site size *n* of 11−14 was found for all poly(A) lengths, which is close to the minimal site size *m* found for binding to oligo(A). The data are discussed with respect to the previous observation of two different forms of the poly(A)−PABPN1 complex.

The 3′ ends of almost all eukaryotic mRNAs are formed by a processing reaction in which the mRNA precursor is first cleaved endonucleolytically and then a poly(A) tail is added (for review see refs *1*−*3*). The poly(A) tail influences nearly all aspects of mRNA metabolism: nucleocytoplasmatic transport (*4*), translation (*5*), and turnover (*6*). A large complex of polypeptides is necessary to reconstitute the complete cleavage and polyadenylation reaction in vitro. In mammalian cells, the central player is the heterotetrameric cleavage and polyadenylation specificity factor (CPSF),[1] which binds directly to the AAUAAA motif of the precursor mRNA and is essential for both the cleavage and the polyadenylation reaction (*7*−*9*). At least three more heterooligomeric proteins are essential for cleavage but play no role in polyadenylation. The enzyme catalyzing polyadenylation, poly(A) polymerase, is nearly inactive on its own and depends on CPSF to perform AAUAAA-dependent polyadenylation (*10*−*12*). A third protein involved in polyadenylation is the nuclear poly(A) binding protein (PABPN1)[2] (*13*, *14*). It binds to the nascent poly(A) tail and, like CPSF, stimulates poly(A) polymerase. Both PABPN1 and CPSF appear to act by enhancing the binding of poly(A) polymerase to its RNA substrate, thus increasing the processivity of the polyadenylation reaction. Whereas poly(A) polymerase alone acts distributively, the addition of either CPSF or PABPN1 results in slight processivity. Full processivity is only reached in the presence of both stimulating factors; in this case a complete poly(A) tail can be synthesized without dissociation of the polymerase (*14*−*16*).

The processive reaction proceeds until the poly(A) tail has been elongated to about 250 adenylates. Further elongation is distributive and therefore slow. This implies that a fully polyadenylated RNA is not able to maintain a stable CPSF−PAP−PABPN1 complex (*16*). In vivo, newly synthesized mRNAs also possess poly(A) tails of 200−300 adenylates (*17*). Thus, the in vitro system reproduces the same tail length control that is observed in vivo. This length control is not based on a kinetic mechanism but on a real measurement of tail length, as substrates with preformed poly(A) tails of different lengths are always elongated processively to the normal length of 250 adenylates (*16*). While the molecular mechanism of tail length control is not known, PABPN1 is supposed to be involved in the length measurement, as it can cover the poly(A) tail stoichiometrically. PABPN1 has a molecular mass of 33 kDa (*13*). Mutagenesis experiments demonstrated that both the RNP domain in the middle of the protein and the arginine-rich C-terminal domain contribute to RNA binding.[3] Binding is specific for purine polyribonucleotides with a marginal preference for poly(A) versus poly(G).

† This work was supported by grants from the Deutsche Forschungsgemeinschaft to S.M. and from the Fonds der Chemischen Industrie to E.W.

* Corresponding author. E-mail: smeyer@biochemtech.uni-halle.de.
‡ Martin-Luther-Universität Halle-Wittenberg.
§ Medizinische Hochschule Hannover.

[1] Abbreviations: CPSF, cleavage and polyadenylation specificity factor; nt, nucleotides; PABPN1, nuclear poly(A) binding protein; RNP, ribonucleoprotein.

[2] The protein was initially described as poly(A) binding protein II (PAB II; accession number X9969 for the bovine cDNA sequence) (*13*). When the human gene was cloned, it was referred to as poly(A) binding protein 2 (PABP2) (*14*). More recently, the NCBI database and the Human Genome Organization nomenclature committee have been using the name poly(A) binding protein, nuclear 1 (PABPN1), for the human protein.

[3] Kühn, Nemeth, Meyer, and Wahle, manuscript in preparation.

10.1021/bi0160866 CCC: $22.00
Published on Web 04/18/2002

Complexes formed between saturating amounts of PABPN1 and high molecular weight poly(A) were recently examined by electron microscopy and scanning force microscopy (*18*). A dynamic structure was observed that showed an equilibrium between a linear filament and a compact particle. The particles reached their maximum size of 21 nm in diameter when PABPN1 was bound to $A_{200-300}$ as opposed to shorter polynucleotides. Complexes of PABPN1 with A_{600} and $A_{\geq 1000}$ showed several discrete-sized 21 nm particles which appeared as "beads on a string". The particle apparently ceased to grow in size with poly(A) molecules exceeding 300 nt in length, and hence particle formation by PABPN1 was most likely self-limiting. As the particle contains approximately the length of a completed poly(A) tail, it was proposed that this dynamic structure may function as a molecular ruler to determine the length of the poly(A) tail. The filament−particle equilibrium was also influenced by the ratio of protein to poly(A). At subsaturating concentrations of PABPN1, a mixture of filaments and particles was found, but as the protein concentration approached saturating levels, the full-sized particles dominated. Because maximum-sized particles were not observed until almost saturating amounts of PABPN1 were added, it was concluded that PABPN1 does not bind to poly(A) with strong cooperativity. This conclusion was supported by gel mobility shift and selection experiments, which also suggested that the full-size particle was not significantly more stable than complexes assembled on poly(A) too short to form 21 nm particles or complexes containing less than saturating amounts of PABPN1 (*18*).

Here we report measurements of poly(A)−PABPN1 binding in equilibrium. By means of fluorescence titration, the thermodynamic parameters K_i (intrinsic association constant), ω (cooperativity), and n (binding site size) of the binding reaction were determined in dependence on poly(A) chain length. We show that there is no significant change in affinity of PABPN1 for poly(A) when the size of the lattice increases from lower than 200 nt to 300−450 nt. The average binding site size was found to be between 11 and 14 for all poly(A) size fractions in different titration modes. This is very close to the minimal binding site size observed on oligo(A). Furthermore, our equilibrium measurements confirm the previous qualitative finding that protein−protein cooperativity is low ($\omega < 50$).

EXPERIMENTAL PROCEDURES

PABPN1 Expression and Purification. Recombinant baculovirus containing the bovine PABPN1 gene with an N-terminal His tag was a kind gift from Gregory Gilmartin (University of Vermont). The virus was amplified in a *Spodoptera frugiperda* cell line (Sf21), cultured in SF 900 II medium supplemented with 10% fetal calf serum, 100 units/mL penicillin, and 100 μg/mL streptomycin (Gibco-BRL). The virus titer was determined with an end-point dilution assay (*19*). For expression of PABPN1, cultivation of Sf21 cells was performed in 1000 mL Erlenmeyer flasks in serum-free SF 900 II medium (400 mL culture volume) at 27 °C and 135 rpm on an orbital shaker. Cultures were infected at a density of about 3×10^6 cells/mL with a multiplicity of infection of 1 and harvested 4 days post infection. Cells were washed with PBS (136 mM NaCl, 2.7 mM KCl, 8.1 mM Na_2HPO_4, 1.5 mM KH_2PO_4, pH 7.2), resuspended in PBS containing 1% Nonidet P-40 and protease inhibitors (1 mM PMSF, 0.2 mM leupeptin, 0.2 mM pepstatin), and incubated for 5 min on ice. After centrifugation for 30 min at 10000*g*, the supernatant (cytoplasmatic extract), which contained most of the recombinant protein, was loaded onto 10 mL of Ni-NTA agarose beads (Qiagen), equilibrated in buffer C (50 mM Tris-HCl, pH 8.0, 10% glycerol, 0.01% Nonidet P-40, and protease inhibitors as above). The resin was washed with buffer C containing 200 mM KCl and 10 mM imidazole, and PABPN1 was eluted with buffer C containing 50 mM KCl and 250 mM imidazole. The eluate was dialyzed against buffer A (50 mM Tris-HCl, pH 8.0, 10% glycerol, 1 mM EDTA, and 0.5 mM DTT) containing 50 mM KCl and loaded onto a 8 mL MonoQ column (Pharmacia) equilibrated in the same buffer. The column was washed with buffer A, and PABPN1 was eluted with a linear salt gradient from 50 to 500 mM KCl in buffer A. The PABPN1-containing fractions, as analyzed by SDS−polyacrylamide gel electrophoresis and Western blotting, were pooled. The final protein concentration was determined by Bradford assay (Bio-Rad) (*20*), densitometric analysis of a Coomassie-stained SDS−polyacrylamide gel (with bovine serum albumin as standard), and absorption at 280 nm, using an extinction coefficient of 18730 M^{-1} cm^{-1}, which was calculated (*21*) from the amino acid sequence (*13*). All three values were in agreement with only a slight difference of ±4%.

Fractionation of Poly(*A*). Heterogeneous poly(A) (Sigma) was separated on a 40 cm long 8% polyacrylamide gel (acrylamide:bisacrylamide, 19:1) containing 8.3 M urea. The gel was cut into horizontal strips of about 2 cm width, and poly(A) was eluted by overnight incubation in elution buffer (10 mM Tris-HCl, pH 8.0, 0.1% SDS, 1 mM EDTA) at 37 °C. Poly(A) was precipitated with 0.3 M sodium acetate and 2.5 volumes of ethanol. The dried precipitate was dissolved in 10 mM Tris-HCl, pH 8.0. A small aliquot of each poly(A) fraction was completely hydrolyzed to AMP by treatment with 0.2 N NaOH for 12 h at 37 °C. The resulting AMP concentration was determined from the UV spectrum after neutralization (extinction coefficient at 259 nm of 15400 M^{-1} cm^{-1} (*22*). Comparison to A_{260} of samples before hydrolysis suggests an extinction coefficient for poly(A) of 10540 M^{-1} cm^{-1}. This is in good agreement with $\epsilon_{260} = 10300$ M^{-1} cm^{-1} used by Casas-Finet et al. (*23*) but higher than $\epsilon_{258} = 9800$ M^{-1} cm^{-1} (Pharmacia catalog) used previously (*24*). The poly(A) lengths were determined by labeling of aliquots of each fraction with [γ-^{32}P]ATP and polynucleotide kinase and separation in an 8% polyacrylamide gel containing 8.3 M urea. A DNA size marker was used for calibration. Due to the nonlinear resolution of the preparative polyacrylamide gel, the poly(A) size fractions contained different size distributions. For example, A_{140} ranged from 130 to 150 monomers, A_{275} from 250 to 300, and A_{450} from 400 to 500. Values given in Results are estimated mean values of each fraction.

Preparation of Oligo(*A*). Heterogeneous poly(A) was partially hydrolyzed by alkali treatment (0.2 N NaOH) for 30 min at 37 °C. For precipitation of the resulting short fragments, 0.3 M sodium acetate, 10 mM magnesium acetate, and 3 volumes of ethanol were added. The precipitation mixture was incubated for 30 min at room temperature and centrifuged for 45 min at 14000 rpm. The precipitate was

dissolved in 8.3 M urea and applied to a 20% polyacrylamide gel containing 8.3 M urea. Well-separated bands were visualized by UV shadowing and excised from the gel. Elution and determination of concentrations were done as for poly(A). For length determination, synthetic A_{10} (IBA, Göttingen, Germany) was used as the size marker in a 20% polyacrylamide/urea gel. Synthetic A_{12} for stoichiometric titrations was purchased from IBA (Göttingen, Germany), purified by anion-exchange chromatography (MonoQ, Pharmacia), and concentrated in the speed vac.

Fluorescence Measurements. All fluorescence titrations were performed with a FluoroMax-2 spectrofluorometer (Jobin Yvon Horiba) at 20 °C in a stirred 1.0 × 1.0 cm cuvette. Standard buffer for fluorescence measurements (buffer B) contained 50 mM Tris-HCl, pH 8.0, 100 mM NaCl, 4 mM magnesium acetate, 0.5 mM DTT, and 0.01% Tween 20. For addition of titrant solution, an automatic dispenser (Eppendorf) was mounted on top of the cuvette. The binding reaction was followed by monitoring the fluorescence of the protein ($\lambda_{ex} = 280$ nm, $\lambda_{em} = 335$ nm). Each data point used for the numerical fit was the mean value of at least four emission values, monitored in 10 s intervals. No fluorescence change with time was observed later than 10 s after addition of titrant solution. In normal titrations, the cuvette contained 2 mL of buffer and 5 μM poly(A), and PABPN1 solution was added in 35 steps of 5 μL each. Final protein concentration was about 1 μM. In inverse titrations, the cuvette contained also 2 mL of buffer, but 0.325 μM PABPN1, and poly(A) solution was added in 35 steps of 5 μL each. The final poly(A) concentration was about 11 μM (nucleotides). Inner filter effects due to the absorbance of excitation light should be negligible, since the extinction at excitation wavelength was only 0.02 at the highest poly(A) concentrations. In both types of titrations, data were corrected for dilution of starting concentrations by addition of titrant solution.

Analysis of Fluorescence Data. In the case of poly(A) titrations, thermodynamic parameters were determined directly from the titration curves by fitting of theoretical binding isotherms using the model of Schwarz and Watanabe (*25*) for the binding of a ligand to a linear polymer as described earlier (*26*). A linear term for baseline drift was included into the calculation algorithm. The protein concentrations were not corrected for possible wall adsorption (see below) since it is difficult to determine the actual amount of adsorbed protein in each titration, and the influence of those small variations in protein concentrations resulted in negligible changes in calculated binding parameters.

For oligo(A) the analysis of fluorescence data was performed by a simple double reciprocal plot, because the available amount of oligo(A) was not sufficient to titrate to complete saturation. Assuming a 1:1 stoichiometry for the binding of oligo(A) [O] to PABPN1 [P], the mass action equation is $K_{obs} = [OP]/([O][P])$. A double reciprocal plot of 1/[OP] vs 1/[O], equivalent to a Lineweaver−Burk plot, shows a linear behavior and has an x intercept of $-K_{obs}$. [OP] was expressed as relative fluorescence quenching, and for [O] the total concentration of each oligo(A) was used. The relationship $K_{obs} = (l - m + 1)K_i$ (*27*), where m is the minimal length of oligonucleotide which forms all favorable contacts with the protein, l is the length of oligonucleotide used, and K_i is the intrinsic association constant, allowed the determination of m and K_i from binding data with a series of oligo(A) differing in length. As the equation can be converted into $K_{obs} = K_i l - (m - 1)K_i$, K_{obs} values were plotted against the chain length l; thus the slope of the regression line represented K_i and the x intercept $m - 1$.

Filter-Binding Assay. The binding mix contained, in 50 μL, 50 mM Tris-HCl, pH 8.0, 50 mM NaCl, 0.5 mM EDTA, 10% glycerol, 0.01% Nonidet P-40, 0.2 mg/mL BSA, 0.5 mM DTT, 400 nM ^{32}P-labeled A_{12}, and PABPN1 between 0 and 1.4 μM. After incubation at room temperature for several minutes, 40 μL of each mix was filtered through a nitrocellulose filter. The filter was washed with ice-cold buffer, and the retained radioactivity was counted.

RESULTS

PABPN1 Purification and Characterization. PABPN1 with an N-terminal His tag was expressed in insect cells and purified to electrophoretic homogeneity in two chromatographic steps. The mammalian PABPN1 contains N^G,N^G-dimethylarginine at 13 positions in the C-terminal part of its amino acid sequence. Two additional arginine residues are partially methylated (*28*). The recombinant protein used in this study was examined by mass spectrometry of peptides obtained by protease Lys C digestion. The overall degree of methylation was about 40% compared to the calf thymus protein, and methylation was limited to the C-terminal fragment as expected. Partial amino acid sequencing showed that of arginines 259, 263, 265, 267, and 269, which are dimethylated in the mammalian PABPN1, 259 was dimethylated in the recombinant protein as well, whereas the others were unmethylated. Arginine 238 was partially methylated in mammalian PABPN1 as well as in the recombinant one. Other arginine residues were not examined. Filter-binding assays (*24*) were performed with the purified recombinant PABPN1 in parallel with wild-type PABPN1 from calf thymus. No difference in poly(A) binding was observed, suggesting that neither the histidine tag nor the lack of complete arginine methylation influences binding. A thorough comparison of fully methylated PABPN1 from calf thymus and unmethylated, untagged protein obtained from *Escherichia coli* also showed no difference in RNA binding properties.[3] Furthermore, no difference between recombinant $PABPN1_{His6}$ and wild-type PABPN1 from calf thymus was found in an in vitro polyadenylation assay with respect to processive polyadenylation and length control. The content of active protein in the preparation used during this study was tested by stoichiometric nitrocellulose filter-binding assays with ^{32}P-labeled A_{12}, performed under conditions of tight binding in buffer containing 0.5 mM EDTA and 50 mM NaCl and concentrations high above the K_D (400 nM oligonucleotide and PABPN1, respectively) (data not shown). Under these conditions, titrations of PABPN1 with A_{12} and vice versa revealed a 1:1 stoichiometry of the oligo(A)−PABPN1 complex and 95% active protein. Analytical ultracentrifugation measurements performed under buffer conditions similar to those used in most of the fluorescence titrations (see below) revealed that, at a concentration of 2 μM PABPN1, the monomer content was about 80% (H. Lilie, personal communication). Thus, protein oligomerization should not affect the polynucleotide binding reaction, since the highest protein concentration used in binding studies was 1 μM.

Fluorescence Titration of PABPN1 with Oligo(A). PABPN1, upon excitation at 280 nm, emits fluorescence with a maximum near 335 nm, and the fluorescence is quenched when the protein is bound to oligo(A) or poly(A) (*24*). Under the conditions used here, maximal quenching was 30−40%. Poly(C) binding to PABPN1 could not be detected in nitrocellulose filter-binding assays (*14*), and accordingly a 15-fold higher poly(C) concentration was needed to reach the same fluorescence quenching as with poly(A) (data not shown). In addition to the filter-binding assay described above, a fluorescence titration at high PABPN1 concentrations (0.265 μM) and under buffer conditions promoting tight binding (50 mM Tris-HCl, pH 8.0, 1 mM EDTA, 0.5 mM DTT, 0.01% Tween 20) was performed in order to confirm the content of active protein. Eighty-seven percent of total protein was found to bind to A_{12} under these conditions, assuming stoichiometric binding. For all further calculations, however, the total protein concentration was used. Full activity of the protein was supported by the fact that titrations with two independent protein preparations gave identical results. All subsequent binding experiments described in this study were performed in the presence of Mg^{2+}, and it is important to note that under these conditions the dissociation constant is increased about 20-fold compared to binding reactions performed in the presence of EDTA (*18*). The buffer conditions were similar to those under which particle formation was observed by electron microscopy (*18*). The salt concentration (100 mM NaCl, 4 mM magnesium acetate) was slightly higher, compared to the conditions of the polyadenylation assay (50 mM KCl, 2 mM $MgCl_2$) under which length control is observed (*16*).

For the description of PABPN1 interactions with oligo(A) and poly(A), we follow the terminology of von Hippel and co-workers (*29*). The parameter m is defined as the minimal length of oligonucleotide which forms all favorable contacts with PABPN1. The site size n is the length of oligomer that PABPN1 will "cover" or make unavailable for binding another PABPN1 molecule. The intrinsic association constant, K_i, describes the affinity of the protein for an isolated binding site. The cooperativity parameter, ω, is the (unitless) equilibrium constant for the process of moving a bound ligand from an isolated site to a singly contiguous site or from a singly contiguous site to a doubly contiguous site. For $\omega > 1$, the ligands attract each other and the binding is positively cooperative; for $\omega < 1$, the ligands repel each other and the binding is negatively cooperative; for $\omega = 1$, the binding is noncooperative (*30*).

Titrations of PABPN1 with oligo(A)s varying in length between 8 and 21 nucleotides (Figure 1A) were used to determine m as well as the intrinsic association constant (K_i). Double reciprocal plots of fluorescence titration curves, where the concentration of the PABPN1−oligo(A) complex [OP] was expressed as relative fluorescence quenching (see Experimental Procedures), showed a linear correlation (Figure 1B), consistent with a 1:1 stoichiometry for PABPN1 and oligo(A) up to 21 nt. The x intercepts of the regression lines represent $-K_{obs}$ for each oligomer. When the length of oligomer (l) exceeds m, the number of possible binding sites for PABPN1 increases as a function of chain length, and the apparent affinity K_{obs} increases proportionally according to $K_{obs} = (l - m + 1)K_i$ (*27*). This relationship allowed the determination of m and K_i from the oligo(A) binding data (see Experimental Procedures). Our data resulted in a minimal chain length of $m = 11$ and an intrinsic association constant of $K_i = 1.8 \times 10^6$ M^{-1} (Figure 2).

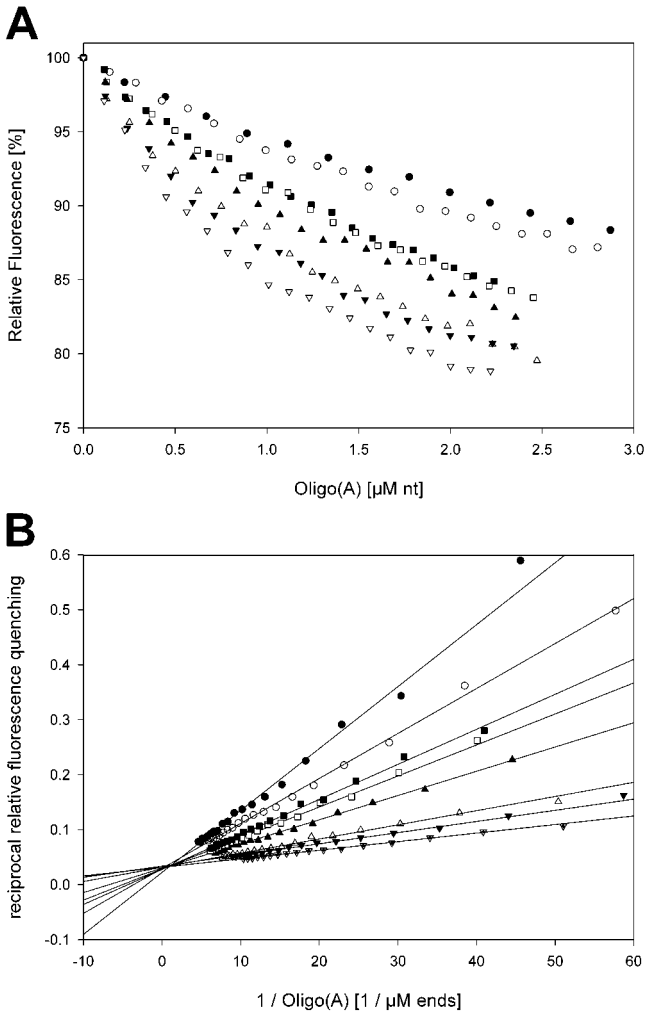

FIGURE 1: Binding of PABPN1 to oligo(A). (A) 0.97 nM PABPN1 was titrated with A_8 (●), A_{11} (○), A_{12} (■), A_{13} (□), A_{14} (▲), A_{17} (△), A_{19} (▼), and A_{21} (▽). (B) Double reciprocal plot of binding curves from (A). Symbols are the same as in (A).

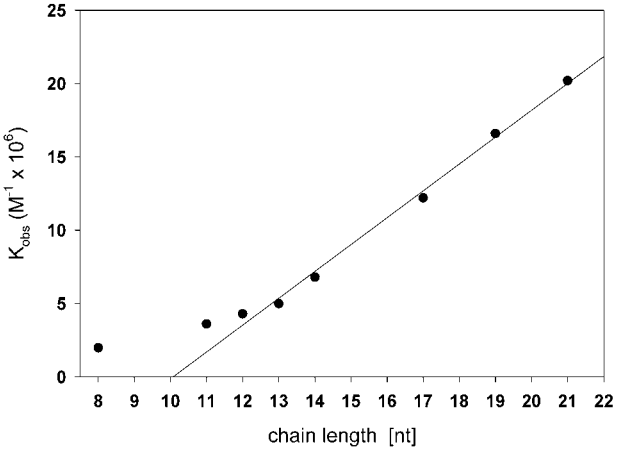

FIGURE 2: Determination of K_i and m. Observed binding constants obtained from double reciprocal plots (Figure 1B) were plotted as a function of chain length. The x intercept ($x = m - 1$) and slope of the regression line are 10 and 1.81×10^6. K_{obs} values of A_8 and A_{11} were omitted from the linear regression.

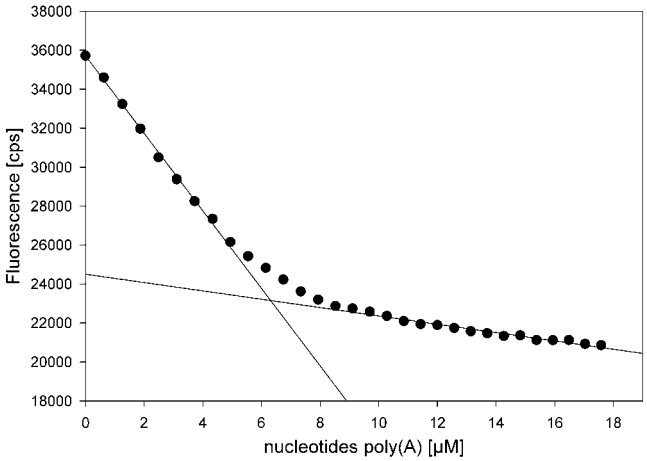

FIGURE 3: Determination of *n* under stoichiometric conditions. PABPN1 (0.666 μM) was titrated in 5 μL steps with A_{205}. Solid lines represent linear regressions of the first and second part of the curve, respectively. The intersection of both lines is at 6.33 μM, resulting in $n = 9.5$.

Determination of n under Stoichiometric Conditions. Several binding experiments were performed in order to obtain the site size *n* independently. Different poly(A) fractions in the range of 140−320 nt were added to PABPN1 at high concentrations (stoichiometric binding conditions). In such titrations a relatively abrupt "break" was observed at the equivalence point (Figure 3), and the molar ratio of poly(A) residues to ligand concentration at that point is equal to the site size *n*. Two different salt conditions were used for this kind of titration: 1 mM EDTA in the absence of salt to promote tight binding or 4 mM Mg acetate/100 mM NaCl, comparable to the conditions in all other titrations described below. Since the dissociation constant is higher in the presence of Mg^{2+} than in the presence of EDTA, as mentioned above, PABPN1 concentrations of 400−660 nM were used in the Mg^{2+}/NaCl containing buffer, compared to only 130−200 nM in the presence of EDTA. From six titrations in the presence of EDTA we obtained a mean value of $n = 11.0 \pm 0.9$, and from five titrations in the presence of Mg^{2+}/NaCl the mean value was 11.0 ± 1.1. Thus, no difference was observed between the two salt conditions.

It should be mentioned that the titrations described above were performed with five different starting concentrations of PABN1 (0.1−0.7 μM). For all concentrations nearly the same stoichiometry was found, providing direct evidence that the fractional fluorescence quenching is linearly correlated to lattice saturation.

Fluorescence Titrations of PABPN1 with Poly(A). Methods to extract basic thermodynamic parameters from binding experiments with polynucleotides, representing continuous lattices of overlapping identical binding sites, have been described (*26*, *31*). In this type of experiment, a constant amount of ligand (PABPN1 in this case) can be titrated with lattice [poly(A)] or vice versa. We performed four titrations in either direction, each with ten different size fractions of poly(A) between 140 and 450 nt in length. Figure 4 shows a titration of A_{270} with PABPN1 ("normal" titration). For comparison, a reference curve is shown in the same graph where identical amounts of protein were added into buffer. The first part of the binding curve (low protein concentrations) showed a shallower slope than the reference curve,

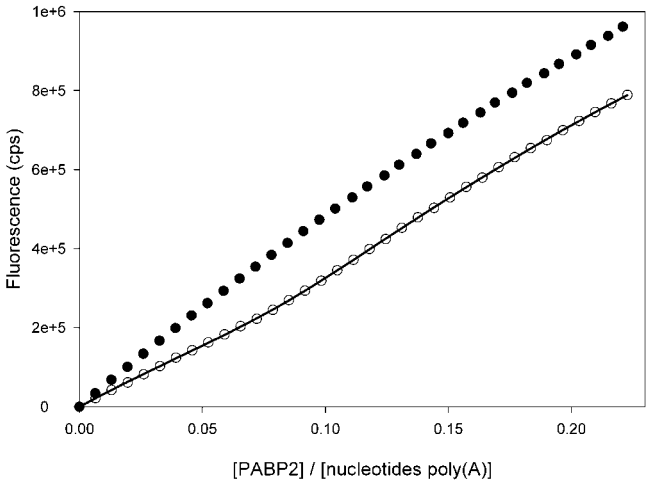

FIGURE 4: Binding of PABPN1 to poly(A). A_{270} (starting concentration 5 μM nucleotides, starting volume 2 mL) was titrated in 5 μL steps with PABPN1 (protein solution contained 13 μM PABPN1) (empty circles). The solid line represents the theoretical binding isotherm calculated using $K_i\omega = 2.9 \times 10^7$ M^{-1} and a binding site size of $n = 11.7$. For comparison, a curve is shown where the same amount of protein was added into the buffer (filled circles).

due to the quenching of fluorescence caused by binding of PABPN1 to poly(A). Upon a further increase of protein concentration, a point was reached at which all poly(A) binding sites were saturated, so that additional protein remained unbound and the increase in fluorescence was the same as in the reference curve. Both the reference curve and the second part of titration curve showed a deviation from expected linearity. This may be due to nonspecific wall adsorption of the protein, since in a control experiment a constant amount of protein showed a fluorescence decrease depending on time and not on illumination of the sample in the cuvette (data not shown). As all measurements were performed with identical time schedules, a linear correction term could be implemented into the fit calculation which corrects for this deviation.

Figure 5 represents an "inverse" titration of a constant amount of PABPN1 with increasing amounts of A_{270}. Increasing saturation of protein with poly(A) resulted in increasing quenching of initial fluorescence until the protein was saturated. A reference curve is shown where the same amount of protein was titrated with buffer instead of poly(A) solution. In all titrations as well as in the buffer control a baseline drift was observed, which was caused by dilution of the fluorophor and, to a smaller extent, by wall adsorption of the protein (see above). When a binding curve was corrected for this loss of protein under the assumption that it was linear with time, no significant change in calculated binding parameters resulted. Thus, such a correction was not done routinely. As the second part of the experimental curve [in which poly(A) was added] had the same slope as the reference curve (in which buffer was added) and the fluorescence loss in the reference curve could be fully accounted for by dilution and wall adsorption of the protein, absorption of the excitation light by poly(A) (extinction of 0.02 at the highest concentration) had no significant effect. Theoretical binding curves were calculated using the parameters K_i, ω, and *n* as well as the fluorescence intensities of the free and bound proteins. A first fit was obtained by

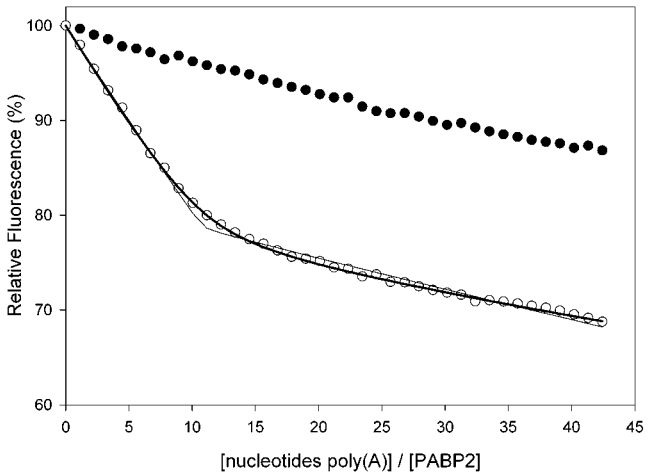

FIGURE 5: Binding of PABPN1 to poly(A). (A) PABPN1 (starting concentration 0.325 μM, starting volume 2 mL) was titrated in 5 μL steps with A_{270} (solution containing 146 μM nucleotides) (empty circles). For comparison, a curve is shown where the same amount of PABPN1 was titrated with buffer (filled circles). The thick line represents the theoretical binding isotherm calculated using $K_i\omega = 3.3 \times 10^7$ M^{-1} and a binding site size of $n = 11.3$. The fine line shows a bad fitting curve calculated using $K_i = 0.6 \times 10^6$ M^{-1}, $\omega = 500$, and $n = 11$.

an iteration algorithm in which all parameters were varied simultaneously. The values obtained for *n* were in the range of 11−14, in good agreement with the independently obtained number. In most inverse titrations and in some of the normal titrations, the correlation coefficient for K_i and ω was 1; in other words, both parameters could not be determined separately. However, in those titrations in which estimates for K_i were obtained, the numbers were in the range of $(0.5-4) \times 10^6$ M^{-1}, in reasonable agreement with the K_i obtained for oligo(A). This justified the assumption that K_i is similar for oligo(A) and poly(A). Cooperativity values obtained from these first calculations were mainly between 10 and 40. The data analysis was repeated with the overall affinity $K_i\omega$ treated as a single variable, and ω was then calculated using $K_i = 1.8 \times 10^6$ M^{-1}, as obtained from the oligo(A) titrations. Calculated binding curves fitted the data accurately as judged on the basis of the differences between data and theoretical curve: Residues were equally distributed, and the average residue was lower than 0.5% of the absolute value. When a curve was calculated in which ω was arbitrarily set to 500, the fit to the data points deteriorated visibly (Figure 5). Smaller changes in ω did not result in visible differences, but the average residue was increased, and more importantly, residues were no longer equally distributed. The results are summarized in Table 1. No significant change in the site size was found with increasing lengths of poly(A). The overall affinity ($K_i\omega$) was also similar for all size classes. The cooperativity parameter ω was low for all size classes of poly(A) (mean value 28.5 ± 14.2). The variability between single measurements of each size fraction was lower for inverse titrations than for normal titrations, possibly due to the large concentration changes of the fluorophor in the latter case. The results from normal and inverse titrations were similar with respect to $K_i\omega$, but lower *n* values were obtained with inverse titrations: *n* was between 12 and 17 in normal titrations (mean value 14.0 ± 2.9) but 10−12 in inverse titrations (mean value 11.3 ± 1.5).

All curves were analyzed a third time using a constant $n = 11$, as obtained from the stoichiometric titrations presented above. In these calculations only $K_i\omega$ was the variable parameter. The resulting theoretical curves fit the data only slightly less precisely compared to the previous analysis: The differences between data and theoretical curve were 0.1−0.5% of the absolute value in the first and 0.15−0.7% in the second analysis. The resulting parameters are shown in Table 2. As expected, similar values for $K_i\omega$ were obtained in the case of inverse titrations, since the value of $n = 11$ is well between 10 and 12, which was obtained in the first analysis. For the normal titrations, somewhat lower values for $K_i\omega$ were obtained (mean value 1.6×10^7 M^{-1}) compared to the first analysis (mean value 5.1×10^7 M^{-1}), since $n = 11$ is not in the range of *n* values obtained from the first analysis.

For the normal titrations, calculations with variable *n* revealed somewhat lower values with poly(A) between 190 and 275 nt in length (*n* between 12 and 14) compared to the longer and shorter poly(A) fractions (*n* between 14 and 17). However, the deviations between single measurements were higher in normal than in inverse titrations (Tables 1 and 2). Thus, the differences in *n* values for different poly(A) fractions may not be significant.

In summary, we found an intrinsic association constant of about 2×10^6 M^{-1} for binding of PABPN1 to oligo(A). The overall affinity found for poly(A) of all size fractions between 140 and 450 nt was consistent with a K_i value in the same range. Protein−protein cooperativity was relatively weak ($\omega \approx 10-40$) and did not change with increasing poly(A) length. The binding site size on poly(A) between 140 and 450 nt in length, determined in stoichiometric titrations, was on average 11. Slightly higher *n* values (*11*−*14*) were found in equilibrium titrations with poly(A) of different length.

DISCUSSION

By means of fluorescence titrations we have characterized the binding of PABPN1 to oligo(A) and poly(A) under equilibrium conditions. The mathematical model of Schwarz and Watanabe (*25*) for the binding of a ligand to a linear polymer was used to determine the thermodynamic binding parameters for different poly(A) size fractions in the range of A_{140} to A_{450}. This and similar models are based on the assumption that two protein monomers interact only if they are bound to the polynucleotide in a contiguous manner, i.e., without gap (nearest-neighbor cooperativity). As PABPN1 can form spherical particles on poly(A) (*18*), it is likely that there are also interactions between protein monomers bound to distant sites. Thus, the model used here may not be entirely appropriate for the interaction considered. Although this means that the numbers obtained have to be interpreted cautiously, it seems very likely that any change in the mode of binding, for example, different modes of binding to polynucleotides of different lengths, would be reflected in a change in one or more of the binding parameters. This type of model has also been found to be useful for other cases of protein−polynucleotide complexes in which non-nearest-neighbor interactions are likely to play a role (*23*, *26*, *32*, *33*).

Within the limits of error, the intrinsic association constant K_i was about 2×10^6 M^{-1}. The binding of PABPN1 to poly-

Table 1: Thermodynamic Parameters Characterizing Binding of PABPN1 to Poly(A) of Increasing Lengths[a]

	normal titrations			inverse titrations		
chain length	$K_i\omega$ ($M^{-1} \times 10^7$)	ω	n	$K_i\omega$ ($M^{-1} \times 10^7$)	ω	n
140	6.3 ± 0.8	34.7 ± 4.7	14.7 ± 2.2	3.4 ± 0.6	18.8 ± 3.5	11.3 ± 1.6
150	5.6 ± 1.6	30.7 ± 8.6	15.6 ± 3.3	3.8 ± 0.6	20.9 ± 3.2	10.4 ± 1.0
165	2.9 ± 0.4	19.9 ± 2.1	11.9 ± 1.5	3.4 ± 1.4	18.7 ± 7.9	9.5 ± 1.1
190	3.8 ± 1.4	17.6 ± 7.6	12.3 ± 2.2	4.1 ± 0.9	23.0 ± 4.8	10.9 ± 0.8
205	6.4 ± 2.3	31.8 ± 12.8	13.4 ± 0.9	5.2 ± 0.7	29.1 ± 3.8	11.3 ± 1.1
230	3.4 ± 1.1	18.8 ± 6.1	12.3 ± 1.4	3.7 ± 1.0	20.6 ± 5.6	11.7 ± 0.8
275	5.5 ± 3.0	30.7 ± 16.9	12.5 ± 0.5	4.0 ± 0.8	22.2 ± 4.2	11.6 ± 0.2
320	5.6 ± 3.9	11.9 ± 21.5	15.3 ± 1.6	4.4 ± 1.2	24.6 ± 6.4	12.8 ± 0.3
370	5.5 ± 2.3	32.6 ± 12.8	14.9 ± 2.9	2.9 ± 1.3	16.1 ± 7.0	11.7 ± 2.8
450	6.1 ± 2.6	33.7 ± 14.7	16.6 ± 5.1	4.4 ± 0.2	24.4 ± 1.2	11.3 ± 1.1

[a] The product $K_i\omega$ and n were used as parameters in the fit procedure. A constant K_i of 1.8×10^6 M^{-1} was used for calculation of ω. Values are mean values of four normal and four inverse titrations, respectively.

Table 2: Thermodynamic Parameters Characterizing Binding of PABPN1 to Poly(A) of Increasing Lengths[a]

	normal titrations		inverse titrations	
chain length	$K_i\omega$ ($M^{-1} \times 10^7$)	ω	$K_i\omega$ ($M^{-1} \times 10^7$)	ω
140	1.2 ± 0.7	6.7 ± 4.2	2.0 ± 0.9	11.1 ± 4.9
150	1.3 ± 0.4	7.2 ± 3.4	3.9 ± 0.1	21.7 ± 0.6
165	1.3 ± 0.2	7.0 ± 3.2	4.7 ± 0.5	26.1 ± 2.8
190	1.3 ± 0.4	7.4 ± 3.5	4.2 ± 1.2	23.2 ± 6.7
205	1.5 ± 0.5	8.4 ± 4.1	2.9 ± 0.6	15.8 ± 3.1
230	2.1 ± 1.2	11.7 ± 7.2	3.0 ± 1.6	16.7 ± 8.8
275	1.8 ± 0.4	9.9 ± 4.3	2.8 ± 0.3	15.6 ± 1.8
320	2.3 ± 1.5	12.6 ± 8.7	1.7 ± 0.4	9.6 ± 2.2
370	1.5 ± 0.3	8.4 ± 3.5	1.7 ± 0.9	9.3 ± 4.9
450	1.6 ± 0.4	8.9 ± 3.9	4.3 ± 1.6	23.9 ± 8.7

[a] The product $K_i\omega$ was used as the variable parameter in the fit procedure; n was set to 11 and kept constant. A K_i of 1.8×10^6 M^{-1} was used for calculation of ω. Titration data are the same as in Table 1.

(A) was enhanced by protein−protein interactions, which were, however, weak. The cooperativity parameter ω was lower than 50; i.e., the net affinity of PABPN1 binding to poly(A) in a contiguous manner is less than 50-fold higher than its affinity for an isolated site. An average binding site size n of ~11 was found. These results are in agreement with previously published data, which were based on less precise measurements under nonequilibrium conditions. When the 20-fold decrease in affinity caused by Mg^{2+} is taken into account, the affinities reported here for a series of oligo(A) are only slightly higher than those determined for a similar series by nitrocellulose filter-binding assays in the presence of EDTA (*24*). A stoichiometric fluorescence titration with unfractionated poly(A) of an average length of 80 nucleotides previously indicated an occluded site size $n = 15$ (*13*, *24*). The minimal site size of $m = 11$ we found is close to the reported value of 9−10 (*13*). The weak cooperativity of the PABPN1−poly(A) interaction described above confirms previous qualitative results (*18*).

While the overall affinity of PABPN1 for poly(A), $K_i\omega$, could be determined accurately, the correlation of the two single parameters, K_i and ω, led to some uncertainty in the determination of both. Fit procedures in which both parameters were varied independently suggested that ω was low (<50) and resulted in K_i values similar to the one independently determined for oligo(A), for which binding is noncooperative. Therefore, a new fit procedure, relying on the assumption that K_i for poly(A) was in fact the same as for oligo(A), was used and led to more uniform estimates of ω (25 ± 12). This degree of cooperativity is certainly low compared to proteins such as hnRNP C ($\omega = 2000-11000$) (*32*) or SSB ($\omega = 10^5$) (*34*). Is the cooperativity of PABPN1 significantly different from $\omega = 1$ (no cooperativity)? The main reason to believe so, in addition to the data presented here, is the fact that certain mutations in PABPN1 can either increase or decrease cooperativity.[3] These experiments also suggest that homotypic protein−protein interactions mediated by the C-terminus of PABPN1 are responsible for cooperative RNA binding. In this respect, PABPN1 can be directly compared to hnRNP A1: This protein has a similar degree of cooperativity ($\omega = 36$) (*35*), and the cooperativity depends on the C-terminal domain (*35*, *36*). Although there is no sequence similarity between the two C-terminal domains, both are arginine-rich, and both contain asymmetric dimethylarginine (*28*, *37*).

As described above, electron microscopy has suggested the existence of two types of PABPN1−poly(A) complexes: filaments and spherical particles (*18*). The dynamic equilibrium between these two forms of the complex was influenced by the ionic strength of the medium: $MgCl_2$ and moderate concentrations of KCl favored formation of spherical particles. As almost all of the titrations reported here were carried out under these buffer conditions, we assume that the poly(A)−PABPN1 complexes in our titrations were predominantly particles. In the EM study, filaments were observed even under buffer conditions favoring particles when subsaturating amounts of PABPN1 were used; filaments disappeared only with saturation of the polynucleotide. Nevertheless, all of our titrations could be fitted accurately with a single set of parameters, indicating a single type of complex under conditions of either excess poly(A) or excess protein. The only small discrepancy was a slightly higher value for n in normal titrations (starting with excess polynucleotide) as compared to inverse titrations (starting with excess protein). This might be taken as evidence for two different types of complexes differing in packing density, possibly a filament at excess polynucleotide and a particle at excess protein. However, several considerations argue that this is probably not the case: The difference between the two n values was barely statistically significant. A change in just n without changes in K and ω does not seem likely. Both types of curves, going from excess protein to excess polynucleotide or vice versa, could be fitted accurately with

just one *n*. Perhaps most strikingly, stoichiometric titrations under conditions favoring particle formation resulted in exactly the same *n* as those under buffer conditions favoring filaments. Thus, the simplest explanation of our results is that filaments do not differ from particles in the way PABPN1 interacts with poly(A); conceivably, the former may be converted to the latter by simply coiling up.

In the EM studies, formation of the full-size particle of 21 nm diameter required poly(A) with a length of 200−300 nucleotides. Smaller particles were formed with shorter chains, and several particles were formed with longer chains. The fluorescence titrations showed that the net affinity ($K_i\omega$) and thus the cooperativity parameter was independent of polynucleotide length, suggesting that the 21 nm particle is not more stable than smaller complexes. This is consistent with previous qualitative results (*18*). The site size *n* was also independent of polynucleotide length.

In summary, our experiments strongly suggest that, under the conditions tested, only a single type of poly(A)−PABPN1 interaction exists, independent of the length of the polynucleotide. The spherical particles seen by electron microscopy and scanning force microscopy (*18*) are thus likely to be formed without changes in the RNA−protein contacts. The full-size 21 nm particle is not detectably stabilized compared to smaller structures. It would be interesting to verify the structure of the poly(A)−PABPN1 complex by methods which directly determine the shape of a macromolecular complex in solution.

ACKNOWLEDGMENT

We thank Peter Rücknagel and Angelika Schierhorn for performing the sequencing and mass spectrometry, Gunter Fischer and Rainer Rudolf for providing instruments, and Gregory Gilmartin for recombinant baculovirus. We also thank Hauke Lilie for performing ultracentrifugations, Franciska Steinhoff for help with experiments, Uwe Kühn for discussions and reading the manuscript, and Peter von Hippel for comments on an earlier version of the manuscript. We are grateful to Jörg Fanghänel for collaboration.

REFERENCES

1. Colgan, D. F., and Manley, J. L. (1997) *Genes Dev. 11*, 2755−2766.
2. Minvielle-Sebastia, L., and Keller, W. (1999) *Curr. Opin. Cell Biol. 11*, 352−357.
3. Wahle, E., and Ruegsegger, U. (1999) *FEMS Microbiol. Rev. 23*, 277−295.
4. Nakielny, S., and Dreyfuss, G. (1999) *Cell 99*, 677−690.
5. Sachs, A. B., and Varani, G. (2000) *Nat. Struct. Biol. 7*, 365−361.
6. Mitchell, P., and Tollervey, D. (2000) *Curr. Opin. Genet. Dev. 10*, 193−198.
7. Bienroth, S., Wahle, E., Suter-Crazzolara, C., and Keller, W. (1991) *J. Biol. Chem. 266*, 19768−19776.
8. Takagaki, Y., Ryner, L. C., and Manley, J. L. (1988) *Cell 52*, 731−742.
9. Keller, W., Bienroth, S., Lang, K. M., and Christofori, G. (1991) *EMBO J. 10*, 4241−4249.
10. Raabe, T., Bollum, F. J., and Manley, J. L. (1991) *Nature 353*, 229−234.
11. Wahle, E. (1991) *J. Biol. Chem. 226*, 3131−3139.
12. Martin, G., Keller, W., and Doublie, S. (2000) *EMBO J. 19*, 4193−4203.
13. Nemeth, A., Krause, S., Blank, D., Jenny, A., Jenö, P., Lustig, A., and Wahle, E. (1995) *Nucleic Acids Res. 23*, 4034−4041.
14. Wahle, E. (1991) *Cell 66*, 759−768.
15. Bienroth, S., Keller, W., and Wahle, E. (1993) *EMBO J. 12*, 585−594.
16. Wahle, E. (1995) *J. Biol. Chem. 270*, 2800−2808.
17. Brawerman, G. (1981) *CRC Crit. Rev. Biochem. 10*, 1−38.
18. Keller, R. W., Kühn, U., Aragon, M., Bornikova, L., Wahle, E., and Bear, D. G. (2000) *J. Mol. Biol. 297*, 569−583.
19. O'Reilly, D. R., Miller, L. K., and Luckow, V. A. (1992) *Baculovirus expression vectors. A laboratory manual*, W. H. Freeman and Co., New York.
20. Bradford, M. M. (1976) *Anal. Biochem. 72*, 248−254.
21. Gill, S. C., and von Hippel, P. H. (1989) *Anal. Biochem. 182*, 319−326.
22. Brewer, J. M., Pesce, A. J., and Ashworth, R. B. (1977) *Experimentelle Methoden in der Biochemie*, Fischer, Stuttgart.
23. Casas-Finet, J. R., Smith, J. D., Kumar, A., Kim, J. G., Wilson, S. H., and Karpe, R. L. (1993) *J. Mol. Biol. 229*, 873−889.
24. Wahle, E., Lustig, A., Jenö, P., and Maurer, P. (1993) *J. Biol. Chem. 268*, 2937−2945.
25. Schwarz, G., and Watanabe, F. (1983) *J. Mol. Biol. 163*, 467−484.
26. Curth, U., Greipel, J., Urbanke, C., and Maass, G. (1993) *Biochemistry 32*, 2585−2591.
27. de Haseth, P. L., and Uhlenbeck, O. C. (1980) *Biochemistry 19*, 6138−6146.
28. Smith, J. J., Rücknagel, K. P., Schierhorn, A., Tang, J., Nemeth, A., Linder, M., Herschman, H. R., and Wahle, E. (1999) *J. Biol. Chem. 274*, 13229−13234.
29. Draper, D. E., and von Hippel, P. H. (1978) *J. Mol. Biol. 122*, 321−338.
30. McGhee, J. D., and von Hippel, P. H. (1974) *J. Mol. Biol 86*, 469−489.
31. Kowalczykowski, S. C., Paul, L. S., Lonberg, N., Newport, J. W., McSwiggen, J. A., and von Hippel, P. H. (1986) *Biochemistry 25*, 1226−1240.
32. McAfee, J. G., Soltaninassab, S. R., Lindsay, M. E., and LeStourgeon, W. M. (1996) *Biochemistry 35*, 1212−1222.
33. Shamoo, Y., Abdul-Manan, N., Patten, A. M., Crawford, J. K., Pellegrini, M. C., and Williams, K. R. (1994) *Biochemistry 33*, 8272−8281.
34. Lohmann, T. M., and Ferrari, M. E. (1994) *Annu. Rev. Biochem. 63*, 527−570.
35. Nadler, S. G., Merrill, B. M., Roberts, W. J., Keating, K. M., Lisbin, M., J., Barnett, S. F., Wilson, S. H., and Williams, K. R. (1991) *Biochemistry 30*, 2968−2976.
36. Kumar, A., Casas-Finet, J. R., Luneau, C. J., Karpel, R., L., Merrill, B. M., Wilson, S. H., and Williams, K. R. (1990) *J. Biol. Chem. 265*, 17094−17100.
37. Kim, S., Merrill, B. M., Rajpurohit, R., Kumar, A., Stone, K. L., Papov, V. V., Schneiders, J. M., Szer, W., Wilson, S. H., Ki Paik, W., and Williams, K. R. (1997) *Biochemistry 36*, 5185−5192.

BI0160866